Published in final edited form as:
Immunity. 2014 October 16; 41(4): 567–578. doi:10.1016/j.immuni.2014.09.016.

The Necroptosis Adaptor RIPK3 Promotes Injury-Induced Cytokine Expression and Tissue Repair

Kenta Moriwaki, **Sakthi Balaji**, **Thomas McQuade**, **Nidhi Malhotra**, **Joonsoo Kang**, and **Francis Ka-Ming Chan***
Department of Pathology, Immunology and Microbiology Program, University of Massachusetts Medical School, Worcester, Massachusetts, 01655, USA

Summary

Programmed necrosis or necroptosis is an inflammatory form of cell death that critically requires the receptor interacting protein kinase 3 (RIPK3). Here we showed that RIPK3 controls a separate, necrosis-independent pathway of inflammation through regulating dendritic cells (DCs) cytokine expression. *Ripk3*$^{-/-}$ bone marrow derived dendritic cells (BMDCs) were highly defective in lipopolysaccharide (LPS)-induced expression of inflammatory cytokines. These effects were caused by impaired NF-κB subunit RelB and p50 activation and caspase 1-mediated processing of interleukin-1β (IL-1β). This DC-specific function of RIPK3 was critical for injury-induced inflammation and tissue repair in response to dextran sodium sulfate (DSS). *Ripk3*$^{-/-}$ mice exhibited an impaired axis of injury-induced IL-1β, IL-23 and IL-22 cytokine cascade, which was partially corrected by adoptive transfer of wild type DCs, but not *Ripk3*$^{-/-}$ DCs. These results reveal an unexpected function of RIPK3 in NF-κB activation, DC biology, innate inflammatory cytokine expression, and injury-induced tissue repair.

Introduction

Programmed necrosis or necroptosis is a non-apoptotic form of cell death with important functions in infectious and sterile inflammation. Similar to apoptosis, necroptosis can be induced by diverse signals including those that stimulate tumor necrosis factor (TNF) receptor-like death receptors, certain toll-like receptors (TLRs) 3 and 4, and the T cell receptor. The receptor interacting protein kinase 3 (RIPK3) is a critical regulator of necroptosis (Moriwaki and Chan, 2013). RIPK3 interacts with its upstream kinase RIPK1

*Correspondence to: Francis Ka-Ming Chan, Department of Pathology, University of Massachusetts Medical School (UMMS), 55 Lake, Avenue North, Worcester, MA 01655, USA, Phone: (508)-856-1664, francis.chan@umassmed.edu.

Author Contributions

K.M. and F.K-M.C. designed the research. K.M. performed the majority of the experimental work. S.B. performed RNA analyses. T.M. performed biochemical experiments. N.M. and J.K. contributed to ILC analyses. K.M. and F.K-M.C. wrote the manuscript. F.K-M. C. supervised the research.

The authors declare no competing financial interests.

via the RIP-homotypic interaction motif (RHIM) to form an amyloid-like complex termed the necrosome that is critical for recruitment of the RIPK3 substrate mixed lineage kinase domain-like (MLKL) (Li et al., 2012). Activated MLKL forms oligomers and translocate to the plasma membrane (Batinic-Haberle et al., 2009; Cai et al., 2014; Chen et al., 2014; Dondelinger et al., 2014). Activated MLKL oligomers eventually cause membrane rupture and the release of danger-associated molecular patterns (DAMPs) to promote inflammatory reactions. RIPK3-mediated necroptosis is optimally triggered when caspase 8 or its adaptor Fas-associated via death domain (FADD) is inactivated. For example, tissue-specific deletion of FADD or caspase 8 in keratinocytes or intestinal epithelium led to spontaneous inflammation that is rescued by inactivation of RIPK3 (Bonnet et al., 2011; Gunther et al., 2011; Welz et al., 2011). These results support the notion that RIPK3-dependent necroptosis is a key driver of inflammatory diseases.

Although the current model predicts that the pro-inflammatory function of RIPK3 is largely due to its role in necroptosis, it is noteworthy that over-expression of RIPK3 in different settings could either enhance or inhibit NF-κB activity (Kaiser et al., 2008; Kasof et al., 2000; Meylan et al., 2004; Sun et al., 1999; Yu et al., 1999). NF-κB is a latent transcription factor that mediates inflammatory cytokine expression in response to TNF-like cytokines and TLR stimulation. Hence, it is possible that RIPK3 facilitates inflammation through necrosis-mediated release of damage-associated molecular patterns (DAMPs) as well as NF-κB induction of inflammatory cytokines. However, TNF- or LPS-induced inhibitor of κB α (IκBα) phosphorylation and degradation in *Ripk3*$^{-/-}$ mouse embryonic fibroblasts (MEFs) and bone marrow derived macrophages (BMDMs) were normal (Newton et al., 2004). As such, it is widely accepted that RIPK3 is dispensable for NF-κB activation.

More recently, RIPK3 has been shown to facilitate pro-IL-1β processing in macrophages and dendritic cells (DCs) lacking cellular inhibitor of apoptosis 1 (cIAP1), cIAP2 and X-linked IAP (XIAP) (Vince et al., 2012) or caspase 8 (Kang et al., 2013). RIPK3-dependent pro-IL-1β processing under these conditions was reported to be independent of necroptosis. Because these observations were made under conditions with artificial inactivation of IAPs or caspase 8, it remains unclear whether RIPK3 can truly control inflammation independent of necroptosis in more physiological settings.

Here, we report that RIPK3 has a critical role in promoting injury-induced reparative inflammation in a mouse model of colitis. We showed that RIPK3 is crucial for induction of an axis of IL-23, IL-1β, and IL-22 in response to injury to the colon. RIPK3 ensured optimal IL-23 and IL-1β expression by promoting nuclear activation of RelB-p50 and caspase 1-mediated pro-IL-1β processing in DCs. Cytokine expression was not affected in *Ripk3*$^{-/-}$ macrophages. Adoptive transfer of wild type BMDCs, but not *Ripk3*$^{-/-}$ or *Ripk3*$^{-/-}$*Casp8*$^{-/-}$ BMDCs, partially restored defective IL-23, IL-1β and IL-22 expression in *Ripk3*$^{-/-}$ mice. These results reveal an unexpected aspect of RIPK3 biology in regulating NF-κB activation, inflammatory cytokine expression and DC functions.

Results

Ripk3$^{-/-}$ mice are highly susceptible to colitis

Mice with conditional deletion of FADD or caspase 8 in the intestinal epithelium suffer from spontaneous colitis that is rescued by ablation of RIPK3, suggesting that RIPK3 promotes inflammatory bowel diseases (Gunther et al., 2011; Welz et al., 2011). We asked if RIPK3 is a promoter of colitis in the presence of intact apoptosis machinery by treating mice with DSS for 7 days, followed by recovery in normal drinking water for 7 days. In *Ripk3*$^{+/+}$ wild type (WT) mice, this treatment led to body weight loss followed by recovery around day 10 as the tissue injury was repaired (Fig. 1A). Contrary to expectation, littermate *Ripk3*$^{-/-}$ mice (KO) developed more severe colitis in response to DSS as determined by weight loss and shortening of the colon (Fig. 1A–B). Although separately housed *Ripk3*$^{+/+}$ and *Ripk3*$^{-/-}$ mice exhibited subtle differences in their intestinal microflora (Fig. S1A, Table S1), they responded similarly to mice that were nursed by the same foster mother from birth or those that were cohoused for four weeks (Fig. S1B–D). These results indicate that *Ripk3*$^{-/-}$ mice do not have transmissible colitogenic microbiota. Moreover, although the difference between *Ripk3*$^{-/-}$ and *Ripk3*$^{+/-}$ was not statistically significant (p=0.0589), *Ripk3*$^{+/-}$ mice showed intermediate body weight loss (Fig. S1E). This indicates that gene dosage of RIPK3 may be important for protection against DSS-induced colitis. Basal colon histology was normal in *Ripk3*$^{-/-}$ mice (Fig. 1C). However, increased injury-induced inflammation and ulcers were apparent in DSS-treated *Ripk3*$^{-/-}$ mice on day 15 (Fig. 1C). Hence, unlike mice with conditional deletion of FADD or caspase 8 in the intestine, RIPK3 limits the extent of chemically induced colitis.

RIPK3 is required for tissue repair, but not DSS-induced tissue injury

The increased colonic injury in *Ripk3*$^{-/-}$ mice was inconsistent with the purported effect of RIPK3 on promoting injury of the colon epithelium. TdT-mediated dUTP nick end labeling (TUNEL) staining, which detects both apoptosis and necrosis (Fig. S2A) (Vanden Berghe et al., 2013), was most prominent in colon epithelial cells on day 4 after DSS treatment when RIPK3 expression was minimal. Importantly, the number of TUNEL^{+} cells was similar in *Ripk3*$^{-/-}$ and *Ripk3*$^{+/+}$ mice (Fig. 2A). However, active caspase 3 staining was absent in the intestine of DSS-treated mice (Fig. S2B), while anti-Fas antibody strongly induced TUNEL and active caspase 3 staining in the liver (Fig. S2C). In addition, mononuclear cells in the lamina propria also did not exhibit increased cell death in response to DSS (Fig. S2D). These results suggest that DSS primarily induces caspase-independent injury in a RIPK3-independent manner.

We found that RIPK3 mRNA expression in the colon was strongly induced by DSS on day 7 and peaked on day 10 when the mice had been weaned from DSS (Fig. 2B). Immunohistochemical staining showed that RIPK3 expression was elevated in the colon epithelium (arrows) as well as in mononuclear cells in the lamina propria (arrowheads) (Fig. 2C, S2E). Because RIPK3 was expressed in mononuclear cell infiltrates and intestinal epithelium, we generated radiation BM chimeras to ascertain the relative contribution of RIPK3 in these compartments (Fig. S2F). *Ripk3*$^{+/+}$ host reconstituted with *Ripk3*$^{-/-}$ BM cells developed similarly severe colitis compared with control *Ripk3*$^{-/-}$ mice receiving

Ripk3$^{-/-}$ BM cells (Fig. 2D, green and red curves). *Ripk3*$^{-/-}$ mice reconstituted with *Ripk3*$^{+/+}$ BM cells showed intermediate body weight loss, suggesting that RIPK3 also had minor role in epithelial tissues (Fig. 2D, blue curve). Measurement of colon length and histological scores confirmed similar pattern of disease severity in the different chimeras (Fig. 2E–F). Hence, in contrast to mice with intestinal epithelium-specific deletion of FADD or caspase 8, RIPK3 expression in hematopoietic cells is critical for limiting the extent of DSS-induced colitis.

RIPK3 is essential for injury-induced IL-1β, IL-23 and IL-22 expression

Increased proliferation of epithelial cells in the crypt is a hallmark of injury-induced repair response (Iizuka and Konno, 2011). We found that cell proliferation in the epithelial crypts as measured by Ki67 staining was reduced in *Ripk3*$^{-/-}$ mice (Fig. 3A). Moreover, expression of repair-associated inflammatory cytokines such as IL-6, cyclooxygenase-2 (Cox2), and epithelial growth factor receptor ligand Epiregulin (Ereg) was also reduced in the colon of *Ripk3*$^{-/-}$ mice (Fig. 3B–C and S3A) (Brandl et al., 2010; Fukata et al., 2006; Grivennikov et al., 2009). Since the numbers of T cells, macrophages and DCs recruited to the inflamed intestine were similar between *Ripk3*$^{-/-}$ and *Ripk3*$^{+/+}$ mice on day 7 (Fig. 3D–E, Fig. S3B), the reduced cytokine expression and repair-associated proliferation in *Ripk3*$^{-/-}$ mice were unlikely to be due to impaired recruitment of immune effectors. Rather, these results implicate that intrinsic defect in cytokine expression by hematopoietic cells is the underlying cause of failed tissue repair response in *Ripk3*$^{-/-}$ mice.

IL-22 is a critical cytokine for tissue repair and homeostasis in the intestine (Cox et al., 2012; Huber et al., 2012; Mizoguchi, 2012; Monteleone et al., 2011; Pickert et al., 2009; Sugimoto et al., 2008; Zenewicz et al., 2008). We found that the expression of IL-22 was severely blunted in *Ripk3*$^{-/-}$ mice (Fig. 4A). However, expression of IL-22 binding protein (IL-22BP) and IL-22 receptor alpha 1 (IL-22RA1) was unaffected in *Ripk3*$^{-/-}$ mice (Fig. S4A). Consistent with diminished IL-22 signaling, expression of the anti-microbial protein Reg3β, a transcriptional target of IL-22, and phosphorylation of signal transducer and activator of transcription 3 (STAT3) were greatly diminished in *Ripk3*$^{-/-}$ mice (Fig. 4B and S4B). Administration of IL-22-Fc, but not isotype control IgG, partially rescued the severe colitis in *Ripk3*$^{-/-}$ mice (Fig. 4C–D). However, although colon length was significantly restored, rescue of body weight loss was not statistically significant. This indicates that while failure to upregulate IL-22 is partly responsible for the susceptibility of *Ripk3*$^{-/-}$ mice to colitis, other factors might also be involved.

Retinoic acid receptor-related orphan receptor gamma t (RORγt) positive innate lymphoid cells (ILCs) are the major producers of IL-22 (Cox et al., 2012; Sawa et al., 2011; Spits and Cupedo, 2012). We found that ILCs developed in normal numbers in *Ripk3*$^{-/-}$ mice (Fig. S4C), and that *Ripk3*$^{-/-}$ ILCs produced IL-22 normally in response to exogenous IL-23 (Fig. 4E–F). This indicates that defective IL-22 expression was due to upstream signals that stimulate IL-22 expression, but not cell-intrinsic ILC defects. IL-23 and IL-β are strong inducers of IL-22 and have been implicated in the pathogenesis of DSS-induced colitis (Becker et al., 2006; Bersudsky et al., 2014; Cox et al., 2012; Lee et al., 2013; Reynders et al., 2011). We found that induction of both cytokines (Fig. 5A, Fig. S5A), but not their

receptors (Fig. S5B), was greatly diminished in the colon of *Ripk3*$^{-/-}$ mice. Significantly, co-administration of IL-23 and IL-1β partially restored IL-22 expression, body weight loss, and colon shortening in *Ripk3*$^{-/-}$ mice (Fig. 5B–D). By contrast, neither cytokine alone was sufficient to ameliorate colitis in *Ripk3*$^{-/-}$ mice (Fig. S5C–F). Hence, an impaired IL-23, IL-1β, and IL-22 axis contributes to the severe colitis in *Ripk3*$^{-/-}$ mice.

RIPK3 is required for cytokine expression in DCs, but not macrophages

DCs and macrophages are powerful sentinels of the immune system that control many aspects of inflammation through cytokine production including IL-1β and IL-23. We used LPS, a TLR4 ligand, to mimic stimulation of DCs and macrophages by commensal bacteria during intestinal injury. LPS-induced expression of IL-23, IL-1β, TNF and monocyte chemotactic protein-1 (MCP-1) was severely inhibited in *Ripk3*$^{-/-}$ BMDCs (Fig. 6A and S6A–B). This is in contrast to *Ripk3*$^{-/-}$ BMDMs, which produced normal amounts of cytokines in response to LPS (Fig. S6C–D). The reduced cytokine expression in *Ripk3*$^{-/-}$ BMDCs was not caused by reduced release of DAMPs, since neither *Ripk3*$^{+/+}$ nor *Ripk3*$^{-/-}$ BMDCs exhibited appreciable cell death in response to LPS alone (Fig. S6E). By contrast, *Ripk3*$^{-/-}$ BMDCs were resistant to LPS and pancaspase inhibitor z-VAD-fmk induced necrosis as expected (Fig. S6E). In addition, supernatants from necrotic cells induced by repeated freeze-thaw cycles did not affect LPS-induced cytokine expression by BMDCs (Fig. S6F). Moreover, while RIPK3- and RIPK1-specific kinase inhibitors blocked necroptosis (Fig. S6G), they did not suppress LPS-induced cytokine expression by BMDCs (Fig. S6H–I). Hence, unlike necroptosis, the kinase activities of RIPK1 and RIPK3 are dispensable for LPS-induced cytokine expression. These results also reinforces the notion that defective necrosis does not contribute to the blunted cytokine expression by *Ripk3*$^{-/-}$ BMDCs.

To test whether defective cytokine expression by DCs is functionally relevant to colitis induction in *Ripk3*$^{-/-}$ mice, we adoptively transferred *Ripk3*$^{+/+}$ or *Ripk3*$^{-/-}$ BMDCs into DSS-treated *Ripk3*$^{-/-}$ mice. IL-22, IL-23p19, and IL-1β expression was significantly restored by *Ripk3*$^{+/+}$, but not by *Ripk3*$^{-/-}$ BMDCs (Fig. 6B). Because DCs developed normally in the lamina propria of *Ripk3*$^{-/-}$ mice (Fig. 3E), these results strongly support the notion that RIPK3 expression enables DCs to sense and to respond to intestinal injury through expression of IL-23 and IL-1β.

RIPK3 controls RelB-p50 and caspase 1 activation in BMDCs

NF-κB is the major driver for expression of many of the cytokines that were defective in *Ripk3*$^{-/-}$ mice and BMDCs (Oeckinghaus and Ghosh, 2009). Previous studies with *Ripk3*$^{-/-}$ fibroblasts and BMDMs showed that RIPK3 was dispensable for IκBα phosphorylation and degradation (Newton et al., 2004). Consistent with this early report, the initial LPS-induced phosphorylation and degradation of IκBα and IκBε were normal in *Ripk3*$^{-/-}$ BMDCs (Fig. 6C and S6J). The slightly higher basal expression of IκBε in *Ripk3*$^{-/-}$ BMDCs may contribute to the impaired RelB-p50 nuclear translocation. Moreover, LPS-induced phosphorylation of the upstream kinases of IκB, IKKα and IKKβ, was normal in *Ripk3*$^{-/-}$ BMDCs (Fig. S6J). In addition, activation of the Mitogen-activated protein (MAP) kinases extracellular signal regulated kinase (Erk) and c-Jun N-terminal kinase (JNK) was not

decreased in *Ripk3*$^{-/-}$ BMDCs (Fig. S6J). Although the initial IκBα phosphorylation and degradation was unchanged, IκBα phosphorylation was greatly diminished at 2 and 6 hours, and NF-κB dependent re-expression of IκBα at 6 hours was impaired in *Ripk3*$^{-/-}$ BMDCs (Fig. 6C, lanes 7 and 14). The late impairment of NF-κB activation might be due to reduced autocrine TNF signaling or defects in NF-κB activation downstream of IκBα. Basal and LPS-induced nuclear translocation of RelB and p50 was diminished in *Ripk3*$^{-/-}$ BMDCs (Fig. 6D). Quantification by FlowSight analysis confirmed that the percentages of *Ripk3*$^{-/-}$ BMDCs with RelB nuclear translocation was significantly reduced compared to *Ripk3*$^{+/+}$ BMDCs (Fig. 6E). By contrast, nuclear RelA and p52 were unaffected in *Ripk3*$^{-/-}$ BMDCs (Fig. 6D). Nuclear cRel was rather slightly increased in *Ripk3*$^{-/-}$ BMDCs. Immunodepletion followed by electrophoretic mobility shift assay (EMSA) showed that nuclear DNA binding activity of the RelB-p50 dimer, but not RelA-p50, was strongly reduced in *Ripk3*$^{-/-}$ BMDCs (Fig. S6K). Unlike LPS, TNF-induced nuclear translocation of RelB and p50, and IL-23 expression were normal in *Ripk3*$^{-/-}$ BMDCs (Fig. S6L). These results are consistent with published report that RelB regulates expression of IL-23p19, TNF, and IL-1β in BMDCs downstream of TLRs (Shih et al., 2012). In contrast, expression of IL-12p35, a c-Rel regulated cytokine (Shih et al., 2012), was normal in *Ripk3*$^{-/-}$ BMDCs (Fig. S6M). Collectively, these results strongly support the notion that RIPK3 specifically regulates expression of a specific set of cytokines in BMDCs through regulating RelB-p50 activation.

RelB is a “non-canonical” NF-κB subunit that dimerizes with p52 and is normally regulated through processing of p100 into p52 (Oeckinghaus and Ghosh, 2009). However, in DCs, RelB forms dimer with p50 and is regulated through binding to IκB proteins in a “canonical” manner (Fig. 6F) (Shih et al., 2012). Because RelB and RIPK3 were highly expressed in BMDCs compared to BMDMs (Fig. S6N), the DC-specific function of RIPK3 may be explained by RIPK3-specific effects on RelB. Reactive oxygen species (ROS) are known to regulate NF-κB nuclear translocation and activation (Morgan and Liu, 2011). Because RIPK3 is a strong inducer of ROS downstream of TNFR and TLRs (Cho et al., 2009; Lushchak, 2012; Vince et al., 2012), we tested the role of ROS in RelB-p50 nuclear translocation. Indeed, we found that LPS stimulated ROS production in *Ripk3*$^{+/+}$, but not *Ripk3*$^{-/-}$ BMDCs (Fig. 6G). The ROS scavengers *N*-acetyl cysteine (NAC) and superoxide dismutase (SOD) mimetic MnTBAP inhibited LPS-induced accumulation of nuclear RelB and p50, but had no effects on nuclear RelA, c-Rel and p52 (Fig. 6H–I and S6O). In contrast, the vitamin E analog Trolox had no effect on RelB or p50 nuclear translocation (Fig. S6O). These results suggest that RIPK3 regulates RelB-p50 nuclear translocation in BMDCs through the induction of ROS.

Although mature IL-1β secretion was completely abrogated (Fig. 6A), IL-1β mRNA was still induced more than 100-fold in *Ripk3*$^{-/-}$ BMDCs (Fig. 7A). Consistent with the strong IL-1β mRNA expression, LPS-induced pro-IL-1β protein expression was normal in *Ripk3*$^{-/-}$ cell lysates (Fig. 7B, top panel). Mature IL-1β secretion requires processing of pro-IL-1β by caspase-1, the active component of the inflammasome (Latz et al., 2013). In DCs, however, LPS alone was sufficient to induce a low amount of caspase 1-dependent IL-1β secretion in the absence of a second inflammasome activating signal (Fig. 7C) (He et al., 2013). This low amount of LPS-induced caspase-1 activation as measured by cleavage into the p10 fragment was abolished in *Ripk3*$^{-/-}$ BMDCs (Fig. 7B). Reduced IL-1β secretion and caspase 1

activation were also observed in *Ripk3*$^{-/-}$ BMDCs when the inflammasome is activated by ATP (Fig. S7A). However, defective IL-1β expression did not contribute to impaired NF-κB activation and cytokine expression in *Ripk3*$^{-/-}$ BMDCs, since neither the caspase 1 inhibitor z-YVAD-fmk, which greatly reduced mature IL-1β secretion (Fig. 7C), nor the IL-1R antagonist Anakinra (Fig. 7D), affected LPS-induced cytokine expression (Fig. S7B). The antioxidant NAC inhibited caspase-1 activation and IL-1β secretion (Fig. 7E–F) (Vince et al., 2012). Injection of NAC into DSS-treated mice strongly suppressed IL-1β and to a lesser extent IL-23 and IL-22 expression (Fig. S7C). However, Trolox did not affect IL-1β secretion, and MnTBAP actually increased IL-1β secretion (Fig. S7D). Hence, while RIPK3-dependent ROS production may contribute to NF-κB activation, cytokine expression and pro-IL-1β processing in response to intestinal injury, other mechanisms may also be involved.

Genetic evidence indicates that RIPK3-dependent necroptosis and IL-1β secretion are optimally induced by ablation of caspase 8 (Gunther et al., 2011; Kang et al., 2013). Given this relationship, one might speculate that enhanced caspase 8 activation is responsible for the impaired cytokine response in *Ripk3*$^{-/-}$ BMDCs. However, LPS-induced caspase 8 activation was not increased, but rather abrogated in *Ripk3*$^{-/-}$ BMDCs (Fig. S7E). Moreover, IL-1β and IL-23p19 expression was equally defective in *Ripk3*$^{-/-}$*Casp8*$^{-/-}$ BMDCs (Fig. S7F). In fact, LPS-induced IL-23p19 expression was further reduced in *Ripk3*$^{-/-}$*Casp8*$^{-/-}$ BMDCs compared with *Ripk3*$^{-/-}$ BMDCs. Furthermore, *Ripk3*$^{-/-}$*Casp8*$^{-/-}$ BMDCs failed to rescue cytokine expression in DSS-treated *Ripk3*$^{-/-}$ mice (Fig. S7G). Thus, impaired NF-κB activation and pro-IL-1β processing in *Ripk3*$^{-/-}$ BMDCs was not caused by hyper-activation of caspase 8. Rather, our results are consistent with a recent report that caspase 8 has a key role in priming the inflammasome (Allam et al., 2014). Taken together, these results indicate that RIPK3 can promote inflammatory cytokine expression independent of necroptosis. Moreover, this necroptosis-independent activity is critical for injury-induced tissue repair.

Discussion

RIPK3-dependent necrosis is widely believed to contribute to detrimental pathologies. In contrast to this view, we have shown that RIPK3 is profoundly important for injury-induced inflammation and tissue repair in the intestine, in part through an IL-23, IL-1β and IL-22 axis. The role of IL-23 in DSS-induced colitis has been controversial. In one report, *Il23p19*$^{-/-}$ mice developed more severe colitis in response to DSS (Becker et al., 2006). However, another report found that IL-23 and IL-23R could either enhance or inhibit DSS-induced colitis depending on the presence of an intact adaptive immune cell compartment (Cox et al., 2012). Our results indicate that the early induction of IL-23 and IL-1β was crucial for IL-22 expression and initiation of the tissue repair program. It is noteworthy that although IL-22 is important for tissue repair, chronic expression of IL-22 is detrimental to intestinal homeostasis and can promote tumorigenesis (Huber et al., 2012). As such, the timing and duration of cytokine action may dictate the biological outcome and explain the discrepant observations for IL-23 in different studies.

Besides IL-1β, IL-23 and IL-22, the nucleotide-binding domain and leucine-rich repeat containing family, pyrin domain–containing 3 (NLRP3) inflammasome-IL-18-myeloid differentiation primary response gene 88 (Myd88) pathway has also been linked to intestinal tissue repair and protection against DSS-induced colitis. *Il18*$^{-/-}$, *Myd88*$^{-/-}$, *Nlrp3*$^{-/-}$, *Asc*$^{-/-}$ and *Casp1*$^{-/-}$ mice are highly sensitive to DSS-induced colitis (Allen et al., 2010; Dupaul-Chicoine et al., 2010; Elinav et al., 2011; Huber et al., 2012; Salcedo et al., 2010; Zaki et al., 2010). However, since IL-18 is mainly produced by intestinal epithelial cells (Dupaul-Chicoine et al., 2010; Zaki et al., 2010) and IL-18 mRNA expression is moderately increased in *Ripk3*$^{-/-}$ mice, IL-18 is unlikely to contribute to the phenotypes of *Ripk3*$^{-/-}$ mice.

Mechanistically, RIPK3 mediates this unique and unexpected function through two distinct signaling mechanisms: nuclear RelB-p50 translocation and caspase 1-dependent pro-IL-1β processing. In contrast to necroptosis, RIPK3 kinase activity was dispensable for RIPK3-dependent cytokine expression. Rather, ROS may play a role in these non-necrotic RIPK3 signaling functions. Different antioxidants had distinct effects on RIPK3-dependent cytokine expression. For example, unlike NAC, the SOD mimetic MnTBAP blocked LPS-induced RelB-p50, but not caspase 1 activation, while the vitamin E analog Trolox had no effects on LPS-induced cytokine expression. NAC is a broad spectrum antioxidant against hydrogen peroxide and other free radicals such as superoxide, peroxynitrite, hydroxyl radicals, and peroxyl radicals (Lushchak, 2012). By contrast, MnTBAP is specific for peroxynitrite and carbonate radicals, but not superoxide (Batinic-Haberle et al., 2009). Trolox mainly prevents the peroxidation of unsaturated lipids in cell membranes and lipoproteins (Niki, 2014). More work is needed to clearly define the role of ROS in necrosis-independent RIPK3 signaling and why different antioxidants exhibit different effects. Nonetheless, these results show that while the kinase activity of RIPK3 drives necroptosis, the scaffolding function of RIPK3, possibly through ROS production, is crucial for necrosis-independent signaling. Since RIPK3 has been reported to interact with certain mitochondrial enzymes (Wang et al., 2012; Zhang et al., 2009), it is tempting to speculate that RIPK3 stimulates mitochondria oxidative burst to facilitate ROS-dependent signaling.

Sensitivity to DSS-induced colitis is strongly influenced by intestinal microbiota (Elinav et al., 2011). For example, *Il18*$^{-/-}$ mice possess a colitogenic gut microbiota that is transmissible to co-housed mice (Elinav et al., 2011). Metagenomic analysis revealed subtle differences in intestinal microbiota between separately housed *Ripk3*$^{+/+}$ and *Ripk3*$^{-/-}$ mice. For example, the number of bacteroidaceae is decreased while lactobacillaceae is increased in *Ripk3*$^{-/-}$ mice compared to *Ripk3*$^{+/+}$ mice. In fact, variation was observed in mice of same genotype from different cages. However, differences in microbiota is unlikely to contribute to the phenotypes of *Ripk3*$^{-/-}$ mice, since littermates, mice nursed by the same foster mother and co-housed mice exhibited similar sensitivity to DSS. Moreover, adoptive transfer of *Ripk3*$^{+/+}$, but not *Ripk3*$^{-/-}$ DCs partially rescued cytokine expression in *Ripk3*$^{-/-}$ mice, a result that cannot be explained by differences in microbiota. As such, we favor a model in which DC-intrinsic functional differences rather than commensal microbiota dictate the tissue repair response of *Ripk3*$^{-/-}$ mice.

DCs are important sentinels that maintain immune homeostasis through the expression of immuno-modulatory cytokines. Colitis was significantly more severe when DCs were selectively depleted, highlighting the protective role of DCs against colitis (Qualls et al., 2009). We propose that the high RIPK3 and RelB expression in BMDCs, but not BMDMs, explains why RIPK3 is uniquely required for BMDC functions. Importantly, DC subsets in the intestinal lamina propria also highly express RIPK3 similar to that seen in BMDCs (unpublished observation). RIPK3 expression is highly inducible in different immune effectors. Thus, physiological cues that modulate RIPK3 expression may determine not only cellular sensitivity to necrosis, but also cytokine responses by distinct immune effectors.

Experimental Procedures

Animal experiments

All mice were housed in specific pathogen-free facility at UMMS. *Ripk3*$^{-/-}$ mice were backcrossed to C57BL/6J background for more than 10 generations and were confirmed by SNP analyses to be > 99.95% on the C57BL/6J background. Female littermates from *Ripk3*$^{+/-}$ crosses were used for the experiments. After weaning littermates, bedding materials from different cages were mixed twice a week to further minimize the differences in intestinal microbial environment. All animal experiments were approved by the institutional animal care and use committee. To induce colitis, female mice (9–11 weeks) were administered 3% DSS (MP Biomedicals, molecular mass 36,000–50,000 Da) in the drinking water for 7 days, followed by 7 days of regular water. The DSS water was replaced on day 3 and 5. Where indicated, mice were injected intraperitoneally with 50 μg IL-22-Fc (PRO312045), mouse isotype-matched control antibody (10D9) (kind gifts from Dr. Ouyang, Genentech), or recombinant mouse IL-23 (0.5 μg) and/or IL-1β (50 ng) (Biolegend). For DC adoptive transfer experiment, BMDCs were treated with 100 ng/ml LPS for 3 hours and then washed with PBS twice to remove LPS. One million stimulated BMDCs were i.p. injected into DSS-treated mice on day 5. In all animal experiments, body weight was monitored throughout the studies and the weight at the beginning of the experiments was normalized as 100%. *Ripk3*$^{-/-}$*Casp8*$^{-/-}$ mice were obtained from Dr. K Fitzgerald (UMMS).

Histopathology and immunohistochemistry

The entire colon was excised to measure colon length. Distal colons were washed with PBS, fixed in 10% buffered formalin, and embedded in paraffin. Tissue sections were stained with hematoxylin & eosin (H&E). Histology was scored by two independent gastrointestinal pathologists in a blinded manner using a semi-quantitative scoring system as follows: presence of ulcer, 0 = none, 1 = punctate, 2 = minimal, 3 = moderate, 4 = widespread; presence of inflammation, 0 = none, 1 = minimal, 2 = mild, 3 = moderate, 4 = severe; extent of inflammation, 0 = none, 1 = mucosal, 2 = mucosal + submucosal, 3 = mucosal + submucosal + muscle penetrate, 4 = full thickness involvement. Total histopathological score was determined by summation of the scores from each category. Immunohistochemical staining was performed on formalin-fixed paraffin-embedded tissues using rabbit anti-CD3 (Abcam), rat anti-F4/80 (Serotec), rabbit anti-Ki67 (Abcam), rabbit anti-active caspase 3 and rabbit anti-phospho-STAT3 (Tyr 705) (Cell Signaling) antibodies.

Liver section was prepared three hours after i.p. injection of anti-mouse Fas antibody (Jo2; BD Biosciences) at a dose of 0.5 mg/kg body weight into WT mice as positive control for active caspase-3 staining. TUNEL staining was performed using an *in situ* cell death detection kit, POD (Roche) according to the manufacturer's instruction. For CD3 scoring, ten visual fields/lamina propria/colon of 5 mice/group were analyzed. For F4/80 scoring, ten visual fields/colon of 5 mice/group were analyzed. For Ki67 scoring, 6–10 crypts/colon of 3–5 mice/group were analyzed. For TUNEL staining, ten visual fields/colon of 3 mice for control and 7–9 mice for DSS-treated mice were analyzed.

Quantitative PCR (Q-PCR)

Total RNA was extracted from colon tissues or cells using RNeasy kit (Qiagen). cDNA was synthesized using Superscript III (Invitrogen). Real-time PCR analysis using iQ SYBR Green supermix (Bio-Rad laboratories) was performed on C1000 thermal cycler and CFX96 real-time system (Bio-Rad laboratories). Primers used in this study were summarized in Supplemental Experimental Procedures. TATA box binding protein (TBP) was chosen as the internal control for the qPCR experiments out of many housekeeping genes tested (β-actin, glyceraldehyde-3-phosphate dehydrogenase, β-glucuronidase, hydroxymethylbilane synthase, hypoxanthine-guanine phosphoribosyltransferase 1, tubuliln α1, and TBP) because it shows minimal variations among samples (data not shown).

Generation of BM radiation chimera

BM cells were collected from femur and tibia by flushing with RPMI1640 media supplemented with 10% FCS, 2 mM Glutamine, 100 units/ml penicillin, and 100 μg/ml streptomycin. T and B cells were depleted by MACS separation LD columns after staining BM cells with biotin-labeled anti-CD3 (BD Biosciences) and biotin-labeled anti-CD19 (eBiosciences) antibodies followed by streptavidin microbeads (Miltenyi Biotech). Cell suspension containing 2.5×10^6 cells (200 ul) was intravenously injected into the irradiated mice (950 rad). For two weeks post-engraftment, mice were given antibiotic water (Trimethoprim and Sulfamethoxazole). Seven weeks after transplantation, the mice were given 3% DSS and leukocytes were prepared by tail bleeding and stained with FITC-labeled anti-CD45.1 (BD Biosciences) for *Ripk3*$^{+/+}$ cells and Pacific blue-labeled anti-CD45.2 (BioLegend) antibodies for *Ripk3*$^{-/-}$ cells. The cells were analyzed by LSRII (BD Biosciences).

Generation and stimulation of BMDCs and BMDMs

For BMDCs, 10×10^6 BM cells were plated in 10 cm tissue culture dish and cultured for a week with 10 ng/ml GM-CSF (BioLegend) and 5 ng/ml IL-4 (Biosource) in RPMI1640 media supplemented with 10% FCS, 2 mM Glutamine, 100 units/ml penicillin, and 100 μg/ml streptomycin. Fresh GM-CSF and IL-4 were added on day 4. Floating cells were collected, plated out and subjected to subsequent experimental analyses. For BMDMs, 10×10^6 BM cells were plated in 10 cm tissue culture dish and cultured for a week in L929-conditioned media. Fresh L929-conditioned media were added on day 4. Attached macrophages were plated out and subjected to subsequent experimental analyses. Purified LPS from Invivogen was used for all experiments. In some experiments, BMDCs were pretreated with RIPK3 kinase inhibitor GSK'843 (GlaxoSmithKline) (Kaiser et al., 2013),

Necrostatin-1 (Nec-1) (Enzo life sciences), z-YVAD-fmk (Enzo life sciences), *N*-acetyl cysteine (NAC) (Calbiochem), MnTBAP (Enzo life sciences), and Trolox (Enzo life sciences) for an hour prior to LPS stimulation. After stimulation, culture media and cells were used for ELISA, RNA, and protein analyses.

Isolation of lamina propria mononuclear cells (LPMCs) from intestine

Colon was harvested from DDS-treated mice on day 7. After removing feces with PBS, the intestine was longitudinally opened and cut into small pieces. The tissue pieces were incubated in pre-digestion solution (DMEM media supplemented with 4% FCS, 25 mM HEPES, 1.5 mg/ml Dispase II, penicillin, and streptomycin) for 20 minutes at 37°C with slow shaking. After filtering, the residual tissue pieces were subsequently incubated in digestion solution (DMEM media supplemented with 4% FCS, 25 mM HEPES, 0.5 mg/ml Collagenase IV, 1 mg/ml Dispase II, 0.5 mg/ml DNase I, penicillin, and streptomycin) for 20 minutes at 37°C with slow shaking. After filtering, the filtrate was subjected to Percoll density gradient separation. LPMCs at the interphase of the two Percoll solutions were collected and subjected to flow cytometric analysis. The cells were analyzed by LSRII (BD Biosciences). For active caspase-3 and TUNEL stainings, PE active caspase-3 apoptosis kit (BD Biosciences) and In situ fluorescent cell death detection kit (Roche) were used, respectively.

Measurement of cytokine secretion

TNF, MCP1, IL-6, and IL-1β were measured using BD OptEIA ELISA sets (BD Biosciences). IL-23 and IL-22 were measured using Mouse ELISA MAX Deluxe sets (BioLegend).

Statistical analysis

P values were calculated using Mann-Whitney test or two-way repeated measures ANOVA. *P* values lower than 0.05 were considered statistically significant.

Supplementary Material

Refer to Web version on PubMed Central for supplementary material.

Acknowledgments

We thank L. Hwa-Jeong and X. Wang (UMMS) for blind histology scoring, the UMass DERC morphology core for immunohistochemistry, V. Kapoor (UMMS) for technical assistance with the BM chimeras, V. Dixit (Genentech) for *Ripk3*$^{-/-}$ mice, K Fitzgerald (UMMS) for *Ripk3*$^{-/-}$*Casp8*$^{-/-}$ mice, P Gough (GlaxoSmithKline) for RIPK3 kinase inhibitor and W. Ouyang (Genentech) for IL-22-Fc. K.M. was supported by a postdoctoral fellowship from the Uehara Memorial Foundation and the Japan Society for the Promotion of Science. This work is supported by NIH grants AI083497 (F.K-M.C) and AI101301 (J.K.). F.K-M.C. and J.K. are members of the UMass DERC (DK32520).

References

Allam R, Lawlor KE, Yu EC, Mildenhall AL, Moujalled DM, Lewis RS, Ke F, Mason KD, White MJ, Stacey KJ, et al. Mitochondrial apoptosis is dispensable for NLRP3 inflammasome activation but non-apoptotic caspase-8 is required for inflammasome priming. EMBO Rep. 2014; 15:982–990. [PubMed: 24990442]

Allen IC, TeKippe EM, Woodford RM, Uronis JM, Holl EK, Rogers AB, Herfarth HH, Jobin C, Ting JP. The NLRP3 inflammasome functions as a negative regulator of tumorigenesis during colitis-associated cancer. J Exp Med. 2010; 207:1045–1056. [PubMed: 20385749]

Batinic-Haberle I, Cuzzocrea S, Reboucas JS, Ferrer-Sueta G, Mazzon E, Di Paola R, Radi R, Spasojevic I, Benov L, Salvemini D. Pure MnTBAP selectively scavenges peroxynitrite over superoxide: comparison of pure and commercial MnTBAP samples to MnTE-2-PyP in two models of oxidative stress injury, an SOD-specific Escherichia coli model and carrageenan-induced pleurisy. Free Radic Biol Med. 2009; 46:192–201. [PubMed: 19007878]

Becker C, Dornhoff H, Neufert C, Fantini MC, Wirtz S, Huebner S, Nikolaev A, Lehr HA, Murphy AJ, Valenzuela DM, et al. Cutting edge: IL-23 cross-regulates IL-12 production in T cell-dependent experimental colitis. J Immunol. 2006; 177:2760–2764. [PubMed: 16920909]

Bersudsky M, Luski L, Fishman D, White RM, Ziv-Sokolovskaya N, Dotan S, Rider P, Kaplanov I, Aychek T, Dinarello CA, et al. Non-redundant properties of IL-1alpha and IL-1beta during acute colon inflammation in mice. Gut. 2014; 63:598–609. [PubMed: 23793223]

Bonnet MC, Preukschat D, Welz PS, van Loo G, Ermolaeva MA, Bloch W, Haase I, Pasparakis M. The adaptor protein FADD protects epidermal keratinocytes from necroptosis in vivo and prevents skin inflammation. Immunity. 2011; 35:572–582. [PubMed: 22000287]

Brandl K, Sun L, Neppl C, Siggs OM, Le Gall SM, Tomisato W, Li X, Du X, Maennel DN, Blobel CP, Beutler B. MyD88 signaling in nonhematopoietic cells protects mice against induced colitis by regulating specific EGF receptor ligands. Proc Natl Acad Sci U S A. 2010; 107:19967–19972. [PubMed: 21041656]

Cai Z, Jitkaew S, Zhao J, Chiang HC, Choksi S, Liu J, Ward Y, Wu LG, Liu ZG. Plasma membrane translocation of trimerized MLKL protein is required for TNF-induced necroptosis. Nat Cell Biol. 2014; 16:55–65. [PubMed: 24316671]

Chen X, Li W, Ren J, Huang D, He WT, Song Y, Yang C, Zheng X, Chen P, Han J. Translocation of mixed lineage kinase domain-like protein to plasma membrane leads to necrotic cell death. Cell Res. 2014; 24:105–121. [PubMed: 24366341]

Cho YS, Challa S, Moquin D, Genga R, Ray TD, Guildford M, Chan FK. Phosphorylation-driven assembly of the RIP1-RIP3 complex regulates programmed necrosis and virus-induced inflammation. Cell. 2009; 137:1112–1123. [PubMed: 19524513]

Cox JH, Kljavin NM, Ota N, Leonard J, Roose-Girma M, Diehl L, Ouyang W, Ghilardi N. Opposing consequences of IL-23 signaling mediated by innate and adaptive cells in chemically induced colitis in mice. Mucosal Immunol. 2012; 5:99–109. [PubMed: 22089030]

Dondelinger Y, Declercq W, Montessuit S, Roelandt R, Goncalves A, Bruggeman I, Hulpiau P, Weber K, Sehon CA, Marquis RW, et al. MLKL compromises plasma membrane integrity by binding to phosphatidylinositol phosphates. Cell Rep. 2014; 7:971–981. [PubMed: 24813885]

Dupaul-Chicoine J, Yeretssian G, Doiron K, Bergstrom KS, McIntire CR, LeBlanc PM, Meunier C, Turbide C, Gros P, Beauchemin N, et al. Control of intestinal homeostasis, colitis, and colitis-associated colorectal cancer by the inflammatory caspases. Immunity. 2010; 32:367–378. [PubMed: 20226691]

Elinav E, Strowig T, Kau AL, Henao-Mejia J, Thaiss CA, Booth CJ, Peaper DR, Bertin J, Eisenbarth SC, Gordon JI, Flavell RA. NLRP6 inflammasome regulates colonic microbial ecology and risk for colitis. Cell. 2011; 145:745–757. [PubMed: 21565393]

Fukata M, Chen A, Klepper A, Krishnareddy S, Vamadevan AS, Thomas LS, Xu R, Inoue H, Arditi M, Dannenberg AJ, Abreu MT. Cox-2 is regulated by Toll-like receptor-4 (TLR4) signaling: Role in proliferation and apoptosis in the intestine. Gastroenterology. 2006; 131:862–877. [PubMed: 16952555]

Grivennikov S, Karin E, Terzic J, Mucida D, Yu GY, Vallabhapurapu S, Scheller J, Rose-John S, Cheroutre H, Eckmann L, Karin M. IL-6 and Stat3 are required for survival of intestinal epithelial cells and development of colitis-associated cancer. Cancer Cell. 2009; 15:103–113. [PubMed: 19185845]

Gunther C, Martini E, Wittkopf N, Amann K, Weigmann B, Neumann H, Waldner MJ, Hedrick SM, Tenzer S, Neurath MF, Becker C. Caspase-8 regulates TNF-alpha-induced epithelial necroptosis and terminal ileitis. Nature. 2011; 477:335–339. [PubMed: 21921917]

He Y, Franchi L, Nunez G. TLR agonists stimulate Nlrp3-dependent IL-1beta production independently of the purinergic P2X7 receptor in dendritic cells and in vivo. J Immunol. 2013; 190:334–339. [PubMed: 23225887]

Huber S, Gagliani N, Zenewicz LA, Huber FJ, Bosurgi L, Hu B, Hedl M, Zhang W, O'Connor W Jr, Murphy AJ, et al. IL-22BP is regulated by the inflammasome and modulates tumorigenesis in the intestine. Nature. 2012; 491:259–263. [PubMed: 23075849]

Iizuka M, Konno S. Wound healing of intestinal epithelial cells. World J Gastroenterol. 2011; 17:2161–2171. [PubMed: 21633524]

Kaiser WJ, Sridharan H, Huang C, Mandal P, Upton JW, Gough PJ, Sehon CA, Marquis RW, Bertin J, Mocarski ES. Toll-like receptor 3-mediated necrosis via TRIF, RIP3, and MLKL. J Biol Chem. 2013; 288:31268–31279. [PubMed: 24019532]

Kaiser WJ, Upton JW, Mocarski ES. Receptor-interacting protein homotypic interaction motif-dependent control of NF-kappa B activation via the DNA-dependent activator of IFN regulatory factors. J Immunol. 2008; 181:6427–6434. [PubMed: 18941233]

Kang TB, Yang SH, Toth B, Kovalenko A, Wallach D. Caspase-8 blocks kinase RIPK3-mediated activation of the NLRP3 inflammasome. Immunity. 2013; 38:27–40. [PubMed: 23260196]

Kasof GM, Prosser JC, Liu D, Lorenzi MV, Gomes BC. The RIP-like kinase, RIP3, induces apoptosis and NF-kappaB nuclear translocation and localizes to mitochondria. FEBS Lett. 2000; 473:285–291. [PubMed: 10818227]

Latz E, Xiao TS, Stutz A. Activation and regulation of the inflammasomes. Nat Rev Immunol. 2013; 13:397–411. [PubMed: 23702978]

Lee Y, Kumagai Y, Jang MS, Kim JH, Yang BG, Lee EJ, Kim YM, Akira S, Jang MH. Intestinal Lin-c-Kit+ NKp46- CD4- population strongly produces IL-22 upon IL-1beta stimulation. J Immunol. 2013; 190:5296–5305. [PubMed: 23589614]

Li J, McQuade T, Siemer AB, Napetschnig J, Moriwaki K, Hsiao YS, Damko E, Moquin D, Walz T, McDermott A, et al. The RIP1/RIP3 necrosome forms a functional amyloid signaling complex required for programmed necrosis. Cell. 2012; 150:339–350. [PubMed: 22817896]

Lushchak VI. Glutathione homeostasis and functions: potential targets for medical interventions. J Amino Acids. 2012; 2012:736837. [PubMed: 22500213]

Meylan E, Burns K, Hofmann K, Blancheteau V, Martinon F, Kelliher M, Tschopp J. RIP1 is an essential mediator of Toll-like receptor 3-induced NF-kappa B activation. Nat Immunol. 2004; 5:503–507. [PubMed: 15064760]

Mizoguchi A. Healing of intestinal inflammation by IL-22. Inflamm Bowel Dis. 2012; 18:1777–1784. [PubMed: 22359410]

Monteleone I, Rizzo A, Sarra M, Sica G, Sileri P, Biancone L, MacDonald TT, Pallone F, Monteleone G. Aryl hydrocarbon receptor-induced signals up-regulate IL-22 production and inhibit inflammation in the gastrointestinal tract. Gastroenterology. 2011; 141:237–248. 248 e231. [PubMed: 21600206]

Morgan MJ, Liu ZG. Crosstalk of reactive oxygen species and NF-kappaB signaling. Cell Res. 2011; 21:103–115. [PubMed: 21187859]

Moriwaki K, Chan FK. RIP3: a molecular switch for necrosis and inflammation. Genes Dev. 2013; 27:1640–1649. [PubMed: 23913919]

Newton K, Sun X, Dixit VM. Kinase RIP3 is dispensable for normal NF-kappa Bs, signaling by the B-cell and T-cell receptors, tumor necrosis factor receptor 1, and Toll-like receptors 2 and 4. Mol Cell Biol. 2004; 24:1464–1469. [PubMed: 14749364]

Niki E. Role of vitamin E as a lipid-soluble peroxyl radical scavenger: in vitro and in vivo evidence. Free Radic Biol Med. 2014; 66:3–12. [PubMed: 23557727]

Oeckinghaus A, Ghosh S. The NF-kappaB family of transcription factors and its regulation. Cold Spring Harb Perspect Biol. 2009; 1:a000034. [PubMed: 20066092]

Pickert G, Neufert C, Leppkes M, Zheng Y, Wittkopf N, Warntjen M, Lehr HA, Hirth S, Weigmann B, Wirtz S, et al. STAT3 links IL-22 signaling in intestinal epithelial cells to mucosal wound healing. J Exp Med. 2009; 206:1465–1472. [PubMed: 19564350]

Qualls JE, Tuna H, Kaplan AM, Cohen DA. Suppression of experimental colitis in mice by CD11c+ dendritic cells. Inflamm Bowel Dis. 2009; 15:236–247. [PubMed: 18839426]

Reynders A, Yessaad N, Vu Manh TP, Dalod M, Fenis A, Aubry C, Nikitas G, Escaliere B, Renauld JC, Dussurget O, et al. Identity, regulation and in vivo function of gut NKp46+RORgammat+ and NKp46+RORgammat- lymphoid cells. Embo J. 2011; 30:2934–2947. [PubMed: 21685873]

Salcedo R, Worschech A, Cardone M, Jones Y, Gyulai Z, Dai RM, Wang E, Ma W, Haines D, O'HUigin C, et al. MyD88-mediated signaling prevents development of adenocarcinomas of the colon: role of interleukin 18. J Exp Med. 2010; 207:1625–1636. [PubMed: 20624890]

Sawa S, Lochner M, Satoh-Takayama N, Dulauroy S, Berard M, Kleinschek M, Cua D, Di Santo JP, Eberl G. RORgammat+ innate lymphoid cells regulate intestinal homeostasis by integrating negative signals from the symbiotic microbiota. Nat Immunol. 2011; 12:320–326. [PubMed: 21336274]

Shih VF, Davis-Turak J, Macal M, Huang JQ, Ponomarenko J, Kearns JD, Yu T, Fagerlund R, Asagiri M, Zuniga EI, Hoffmann A. Control of RelB during dendritic cell activation integrates canonical and noncanonical NF-kappaB pathways. Nat Immunol. 2012; 13:1162–1170. [PubMed: 23086447]

Spits H, Cupedo T. Innate lymphoid cells: emerging insights in development, lineage relationships, and function. Annu Rev Immunol. 2012; 30:647–675. [PubMed: 22224763]

Sugimoto K, Ogawa A, Mizoguchi E, Shimomura Y, Andoh A, Bhan AK, Blumberg RS, Xavier RJ, Mizoguchi A. IL-22 ameliorates intestinal inflammation in a mouse model of ulcerative colitis. J Clin Invest. 2008; 118:534–544. [PubMed: 18172556]

Sun X, Lee J, Navas T, Baldwin DT, Stewart TA, Dixit VM. RIP3, a novel apoptosis-inducing kinase. J Biol Chem. 1999; 274:16871–16875. [PubMed: 10358032]

Vanden Berghe T, Grootjans S, Goossens V, Dondelinger Y, Krysko DV, Takahashi N, Vandenabeele P. Determination of apoptotic and necrotic cell death in vitro and in vivo. Methods. 2013; 61:117–129. [PubMed: 23473780]

Vince JE, Wong WW, Gentle I, Lawlor KE, Allam R, O'Reilly L, Mason K, Gross O, Ma S, Guarda G, et al. Inhibitor of apoptosis proteins limit RIP3 kinase-dependent interleukin-1 activation. Immunity. 2012; 36:215–227. [PubMed: 22365665]

Wang Z, Jiang H, Chen S, Du F, Wang X. The mitochondrial phosphatase PGAM5 functions at the convergence point of multiple necrotic death pathways. Cell. 2012; 148:228–243. [PubMed: 22265414]

Welz PS, Wullaert A, Vlantis K, Kondylis V, Fernandez-Majada V, Ermolaeva M, Kirsch P, Sterner-Kock A, van Loo G, Pasparakis M. FADD prevents RIP3-mediated epithelial cell necrosis and chronic intestinal inflammation. Nature. 2011; 477:330–334. [PubMed: 21804564]

Yu PW, Huang BC, Shen M, Quast J, Chan E, Xu X, Nolan GP, Payan DG, Luo Y. Identification of RIP3, a RIP-like kinase that activates apoptosis and NFkappaB. Curr Biol. 1999; 9:539–542. [PubMed: 10339433]

Zaki MH, Boyd KL, Vogel P, Kastan MB, Lamkanfi M, Kanneganti TD. The NLRP3 inflammasome protects against loss of epithelial integrity and mortality during experimental colitis. Immunity. 2010; 32:379–391. [PubMed: 20303296]

Zenewicz LA, Yancopoulos GD, Valenzuela DM, Murphy AJ, Stevens S, Flavell RA. Innate and adaptive interleukin-22 protects mice from inflammatory bowel disease. Immunity. 2008; 29:947–957. [PubMed: 19100701]

Zhang DW, Shao J, Lin J, Zhang N, Lu BJ, Lin SC, Dong MQ, Han J. RIP3, an energy metabolism regulator that switches TNF-induced cell death from apoptosis to necrosis. Science. 2009; 325:332–336. [PubMed: 19498109]

Highlights

- RIPK3 limits the extent of injury-induced colitis
- RIPK3 promotes IL-22-mediated tissue repair through IL-23 and IL-1β expression
- RIPK3 facilitates LPS-induced RelB and p50 nuclear translocation in BMDCs
- RIPK3 promotes caspase-1-dependent IL-1β processing in BMDCs

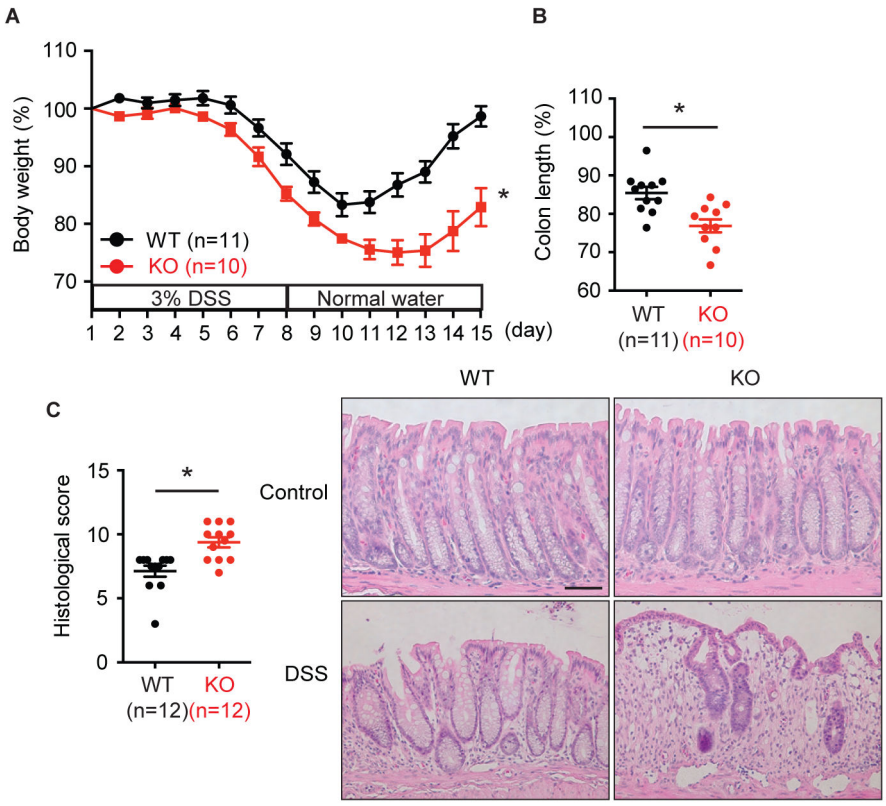

Fig. 1. RIPK3 protects against DSS-induced colitis

(A) Body weight and **(B)** colon length on day 15 of 3% DSS-treated *Ripk3*$^{-/-}$ (KO) and their littermate *Ripk3*$^{+/+}$ (WT) mice. **(C)** Histological score of distal colon of 3% DSS-treated mice on day 15 were measured. Representative microscopic pictures of H&E stained colon from control mice and the mice treated with DSS for 15 days are shown on the right. Scale bar = 75 μm. The number in parentheses represents the number of mice used in each group. Results shown are mean ± SEM. Asterisks: $p < 0.05$. Three independent experiments. See also Figure S1.

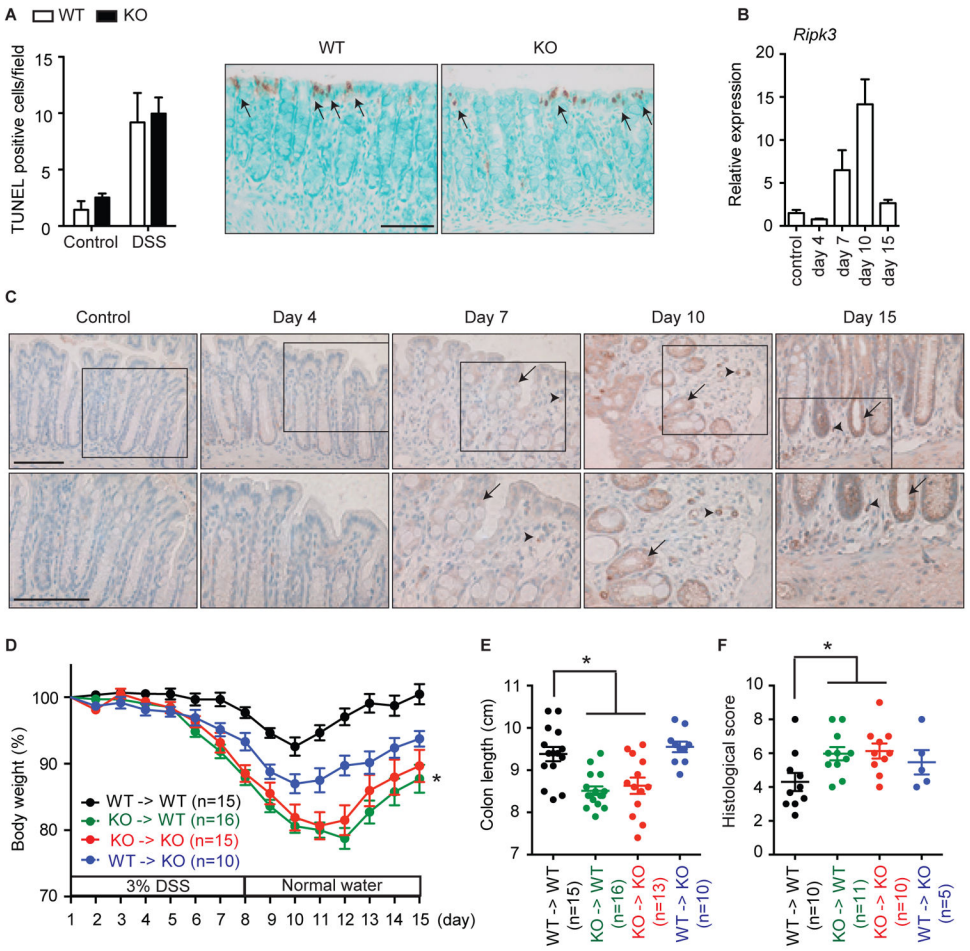

Fig. 2. RIPK3 in hematopoietic cells are required for the protection against DSS-induced colitis

(A) The number of TUNEL$^+$ cells/visual field in colons from control mice and the mice treated with DSS for 4 days was enumerated. Representative pictures of TUNEL staining are shown. Arrows indicate TUNEL-positive cells. **(B)** Relative mRNA expression of *Ripk3* in colon tissues of DSS-treated *Ripk3*$^{+/+}$ mice (n=4–8). **(C)** RIPK3 expression in colon sections. Arrows and arrowheads indicate RIPK3$^+$ colon epithelial cells and mononuclear cells in lamina propria, respectively. Magnified views of the marked areas are shown in lower panels. **(D–F)** Bone marrow chimeras of the indicated genotypes were fed 3% DSS water and **(D)** body weight, **(E)** colon length and **(F)** histological score were measured. The numbers in parentheses represent the number of mice used in each group. White and black bars show *Ripk3*$^{+/+}$ (WT) and *Ripk3*$^{-/-}$ (KO) mice, respectively. Scale bars = 75 μm. Results shown are mean ± SEM. Asterisks: $p < 0.05$ (**D**, green vs black or blue). Three independent experiments. See also Figure S2.

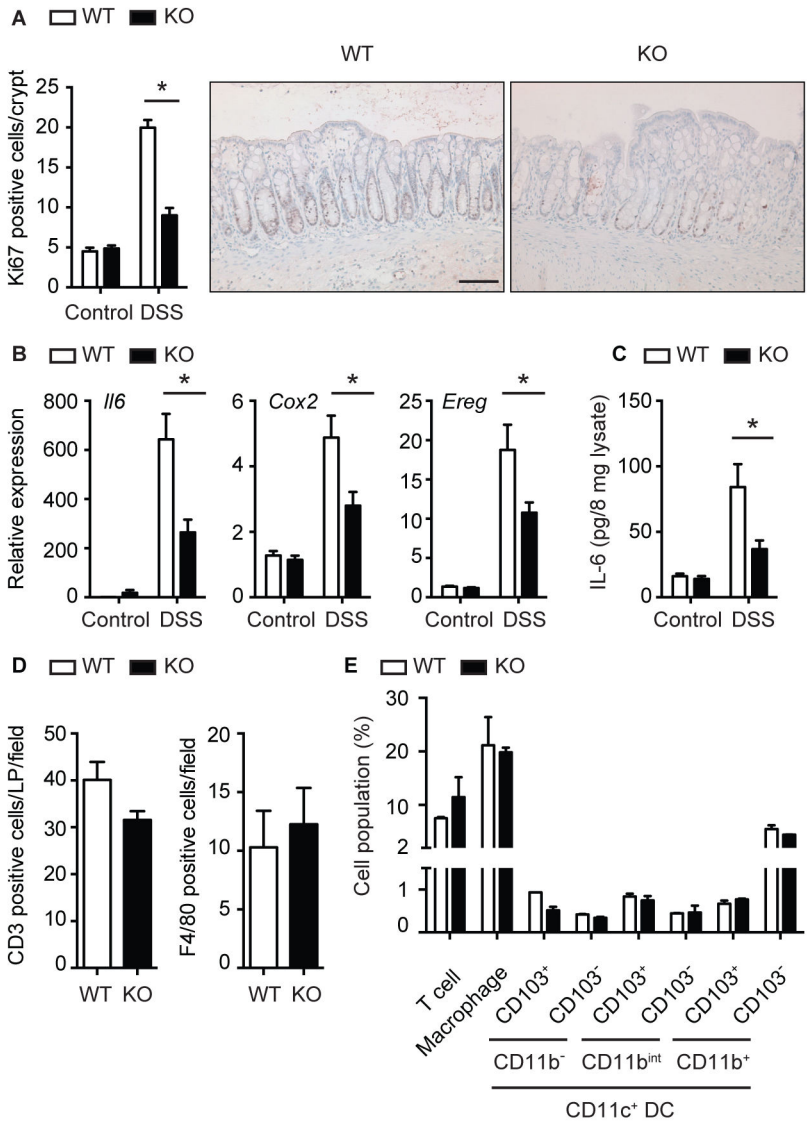

Fig. 3. RIPK3 promotes repair of the intestinal epithelium

(A) The number of Ki67^{+} cells/colon crypt from control mice and the mice treated with DSS for 7 days was enumerated. Representative pictures of Ki67 staining are shown on the right. Scale bars = 75 μm. **(B)** Relative mRNA (n=5–12) and **(C)** protein expression (n=3–6) in DSS-treated *Ripk3*$^{+/+}$ (WT) and *Ripk3*$^{-/-}$ (KO) colon on day 7. **(D)** T cell and macrophage recruitment to the colon after DSS treatment (day 7). **(E)** T cell, macrophage, and DC populations in the colonic lamina after DSS treatment (day 7). CD3^{+} cells and CD3^{-}CD19^{-}CD11c^{-}CD103^{-}CD11b^{+} cells were defined as T cells and macrophages, respectively. CD11c^{+} cells were defined as DCs. The various DC subsets defined by cell surface markers are also shown. Data were obtained from 4 mice for each genotype; 2 mice were pooled. Results shown are mean ± SEM. Asterisks: $p < 0.05$. See also Figure S3.

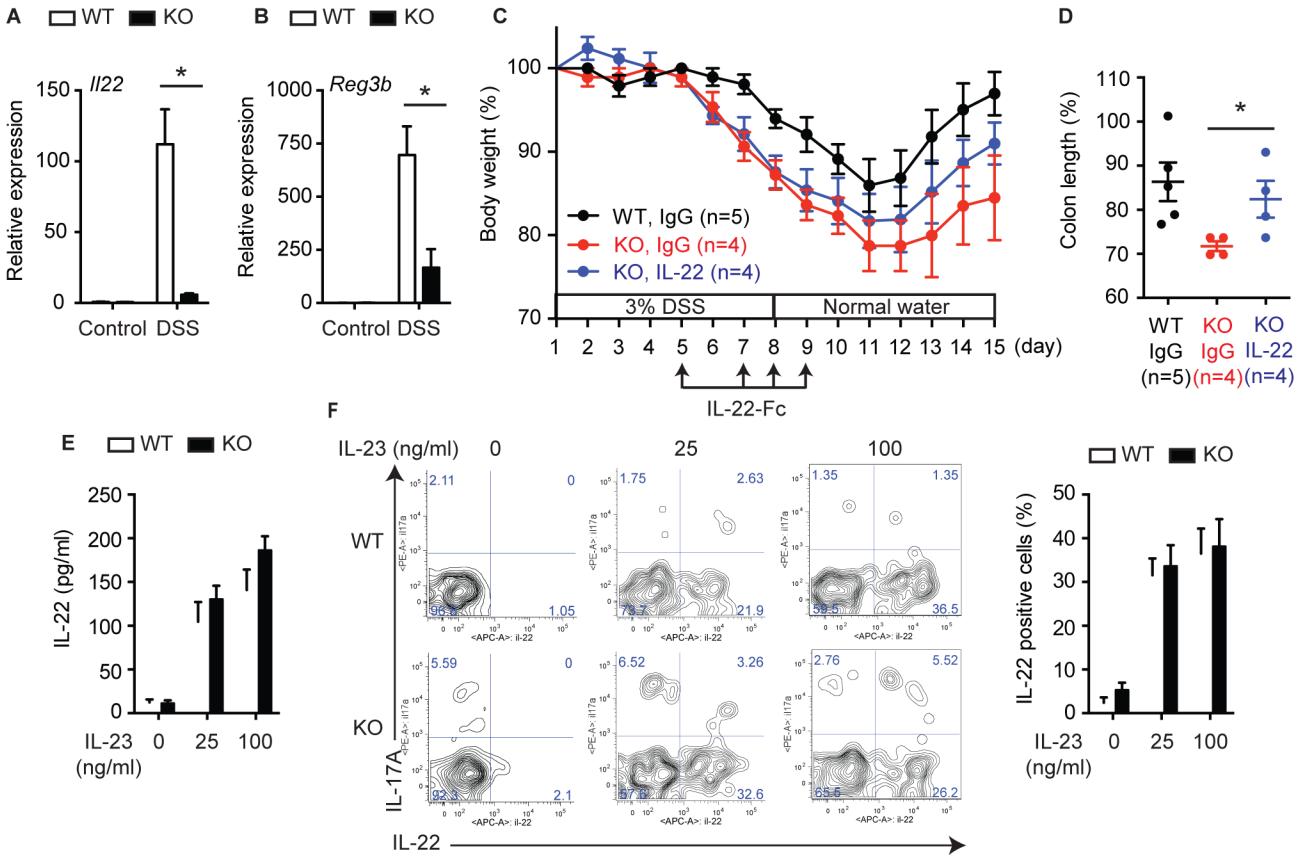

Fig. 4. RIPK3 protects against DSS-induced colitis through IL-22 expression

(A–B) Relative mRNA expression of **(A)** *Il22* and **(B)** *Reg3b* in colon tissues of DSS-treated *Ripk3*$^{+/+}$ (WT) and *Ripk3*$^{-/-}$ (KO) mice (day 7, n=5–12). **(C)** Body weight and **(D)** colon length on day 15 in the mice treated with 50 μg IL-22-Fc or isotype control IgG. The number in parentheses represents the number of mice used in each group. **(E–F)** Splenocytes were stimulated with IL-23 in the presence of PMA and Ionomycin. **(E)** IL-22 expression was determined by ELISA (n=4). **(F)** Representative FACS plots showing IL-22 expression in splenic ILCs (CD3^{-}CD19^{-}CD11b^{-}IL-7R^{+}CD4^{+}CD25^{+} cells). The percentage of IL-22^{+} cells in splenic ILCs is shown on the right (n=4). Results shown are mean ± SEM. Asterisks: $p < 0.05$. See also Figure S4.

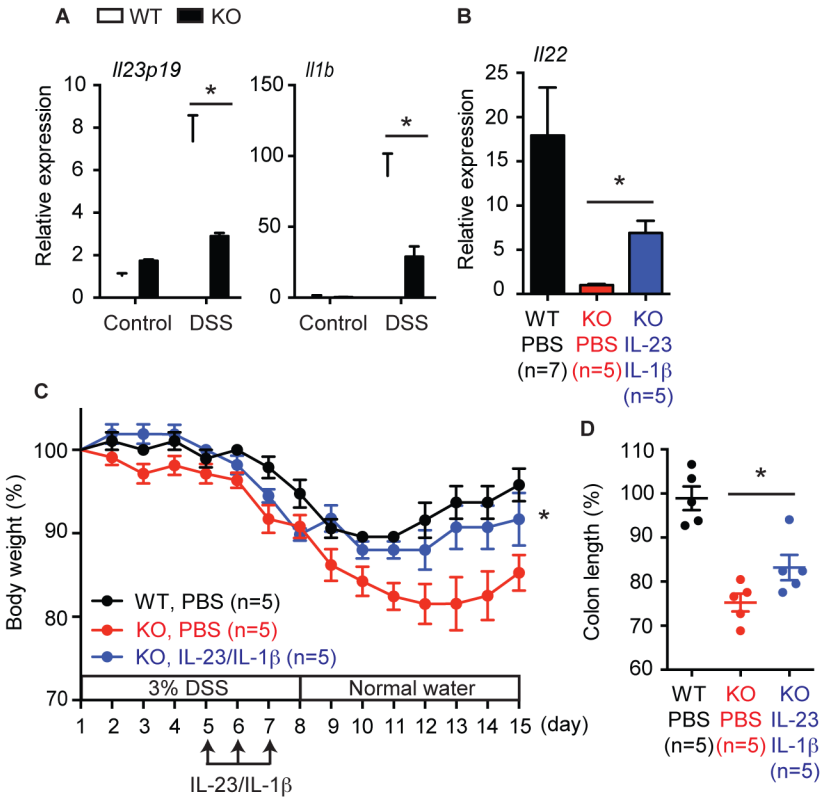

Fig. 5. RIPK3 controls IL-22 expression through IL-23 and IL-1β induction

(A) Relative mRNA expression of *Il23p19* and *Il1b* in colon tissues of DSS-treated *Ripk3*$^{+/+}$ (WT) and *Ripk3*$^{-/-}$ (KO) mice (day 7, n=5–12). **(B)** *Il22* expression on day 7, **(C)** body weight, and **(D)** colon length on day 15 in the mice treated with PBS or IL-1β and IL-23. The number in parentheses represents the number of mice used in each group. Results shown are mean ± SEM. Asterisks: $p < 0.05$ (**C**, blue vs red). See also Figure S5.

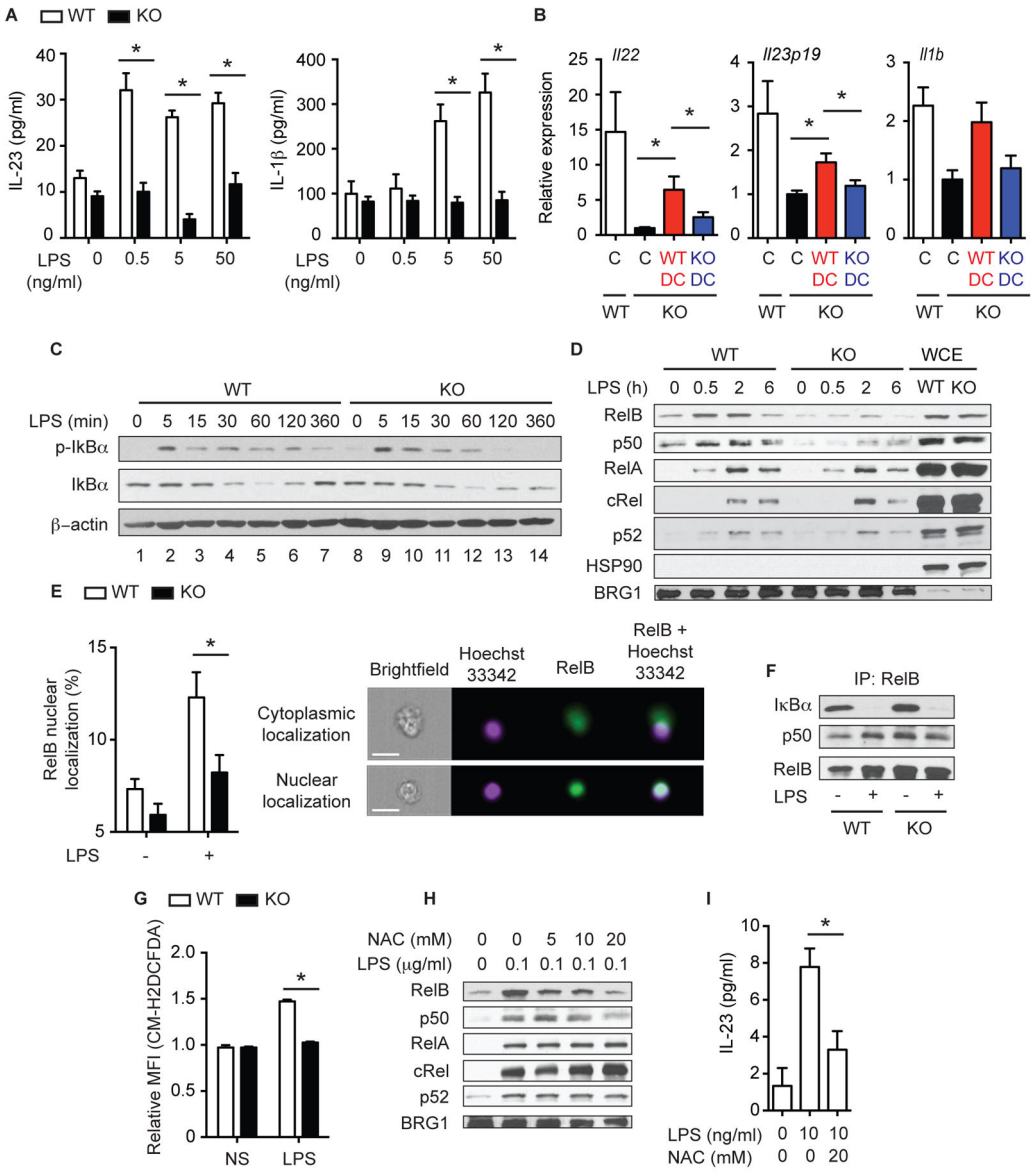

Fig. 6. RIPK3 controls cytokine production in DCs by regulating RelB and p50 nuclear translocation

(A) IL-23 and IL-1β secretion by BMDCs treated with LPS for 6 hours (n=4). **(B)** *Ripk3*$^{+/+}$ (WT: n=10) or *Ripk3*$^{-/-}$ (KO: n=8) BMDCs were injected to *Ripk3*$^{-/-}$ mice on day 5. PBS was injected into control mice (*Ripk3*$^{+/+}$: n=14, *Ripk3*$^{-/-}$: n=8). Cytokine expression in the colon on day7 is shown. Gene expression in *Ripk3*$^{-/-}$ PBS control was defined as 1. C: control. The results were pooled from two independent experiments. **(C)** Whole cell extracts (WCE) and **(D)** nuclear extracts from BMDCs treated with 100 ng/ml LPS were subjected to western blot analyses. p-IκBα = phopho IκBα. **(E)** BMDCs stimulated with 100 ng/ml LPS for 2 hours were subjected to intracellular staining for RelB (n=8). Representative pictures of cytoplasmic (top) and nuclear (bottom) RelB localization is shown on the right. Scale bars = 20 μm. **(F)** WCEs from *Ripk3*$^{+/+}$ and *Ripk3*$^{-/-}$ BMDCs treated with 100 ng/ml LPS for 2 hours were subjected to immunoprecipitation with anti-RelB antibody followed by western

blot analyses. **(G)** Relative mean fluorescence intensity (MFI) of the ROS reactive dye CM-H2DCFDA was measured in BMDCs treated with 100 ng/ml LPS for 6 hours (n=4). **(H)** NF-κB nuclear translocation (2 hours) and **(I)** IL-23 secretion (3 hours, n=4) by *Ripk3*$^{+/+}$ BMDCs treated with LPS in the presence of NAC. Results shown are mean ± SEM. Asterisks: $p < 0.05$. See also Figure S6.

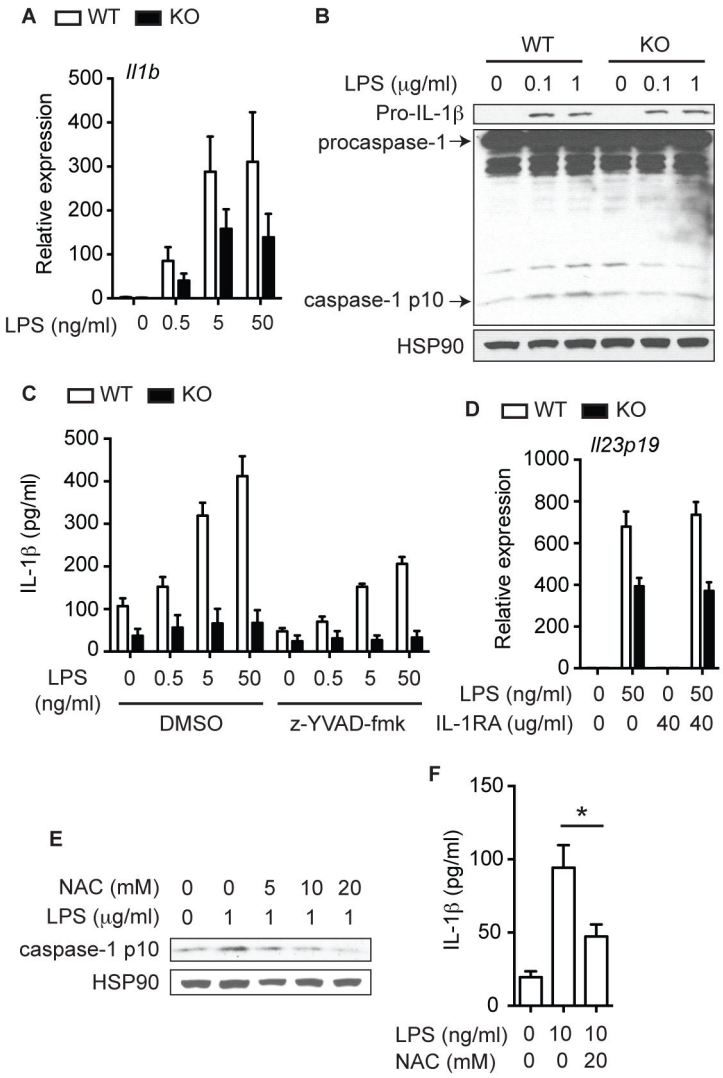

Fig. 7. RIPK3 controls IL-1β secretion in DCs through inflammasome activation

(A) Relative mRNA expression of *Il1b* in *Ripk3*$^{+/+}$ (WT) and *Ripk3*$^{-/-}$ (KO) BMDCs treated with LPS for 6 hours (n=4). **(B)** WCE from BMDCs treated with LPS for an hour was tested by western blot analysis. **(C)** Cytokine expression in BMDCs pretreated with 5 μM z-YVAD-fmk and then stimulated with LPS for 6 hours (n=2). **(D)** Relative *Il23p19* expression in BMDCs pretreated with IL-1RA for an hour and then stimulated with LPS for 6 hours (n=3). **(E)** Caspase 1 activation (1 hour) and **(F)** IL-1β secretion (3 hours, n=4) in *Ripk3*$^{+/+}$ BMDCs treated with LPS in the presence of NAC. Results shown are mean ± SEM. Asterisks: $p < 0.05$. See also Figure S7.